Work Function Study of the Adsorption, Lateral Repulsion, and Fragmentation of CH_3Br on Ru(001)

T. Livneh and M. Asscher*

Department of Physical Chemistry and the Farkas Center for Light Induced Processes, The Hebrew University, Jerusalem 91904, Israel

Received: April 1, 1997; In Final Form: July 9, 1997[⊗]

The chemistry of methyl bromide on Ru(001) has been studied utilizing work function change ($\Delta\varphi$) measurements and temperature-programmed desorption (TPD) in the crystal temperature range of 82−1350 K. Employing a $\Delta\varphi$-TPD mode, chemical changes in the adsorbed state could be detected at temperatures below the onset for desorption. A decrease in work function of 2.15 ± 0.02 V has been measured at the completion of a monolayer coverage, which has been determined to consist of $(3.6 \pm 0.3) \times 10^{14}$ molecules/cm^2, equivalent to $CH_3Br/Ru = 0.22 \pm 0.02$. The onset for C−Br bond cleavage near 125 K was observed. 50% of the initial 1 monolayer methyl bromide molecules decompose to adsorbed methyl and bromine. A low-temperature increase in work function was found to precede dissociation or desorption as coverage increases. This change in work function is discussed in terms of several possible mechanisms, including multiple sites population, molecular rearrangement, and tilt angle, that change with coverage and surface temperature. A thermally activated flipping mechanism in which a fraction of the adsorbate molecules rearrange to adsorb with the methyl group facing the surface is found to be most consistent with the observed results. Sequential dehydrogenation of the methyl fragments, competing with minor methane production at higher coverages, was directly observed by employing the differential work function measurements. The corresponding surface temperature window for each of these decomposition steps has been determined, and the detailed reaction mechanism is discussed. Bromine atoms on Ru(001) were found to decrease the work function by 320 mV at a coverage $Br/Ru = 0.3$, indicating a complex charge redistribution upon adsorption. Deuterium preadsorption, which significantly passivates the surface, has been employed to better understand the various reactivity steps of the hydrocarbon fragments. Finally, work function measurements indicate the presence of strong interactions of the methyl bromide molecules with the metal surface up to the third layer. Alternating contributions to the work function of the first three layers are observed. This is understood in terms of an opposite adsorption geometry in which bromine faces the surface in the first layer, methyl in the second, and bromine again in the third. Upon heating, the third and fourth layers rearrange in a bilayer-like structure before the completion of the fourth layer, leading to higher stability of the combined two layers compared with the third alone. This structure is rather similar to that of methyl bromide in its molecular crystal.

I. Introduction

The chemistry of alkyl halides on metal surfaces has attracted considerable attention in recent years. The importance of these molecules as precursors in many processes in the chemical industry, as models for surface alkylation and in particular their damaging role in atmospheric reactions, has motivated these studies. Under ultrahigh vacuum (UHV) conditions it was possible to compare the reactivity of different methyl halides (X = Cl, Br, I) on several catalytic metal surfaces. Thermal reactivity on most metals (e.g. Al(111),[1] Al(100),[2] Ru (001),[3] Pt(111),[4−8] Pd (111),[9] Cu single crystals,[10−13] and Ag(111)[14,15]) toward C−X bond cleavage has been found to follow the trend I > Br > Cl. Close packed surfaces of the noble metal, tend to dissociate predominantly methyl iodide, while the other methyl halides desorb molecularly. The more reactive surfaces, like Ni(111), can break the methyl−bromide bond as well.[16] When the alkyl chain becomes longer, less reactive halides also thermally dissociate. This is attributed to the higher barrier to desorption, which keeps the molecules on the surface for high enough temperatures to open the dissociative channel.[17]

Methyl halides were studied also as a relatively simple and clean source of methyl radicals on surfaces. Once dissociated the coadsorbed halide was found in most cases to present a relatively minor perturbation on the surface chemistry of the adsorbed methyl group. The interest in the chemistry of these radicals stems from the need to better understand the exact mechanism of decomposition and recombination reactions of C_1 hydrocarbon intermediates on metal surfaces in the heterogeneous catalysis of hydrocarbons in general.[17] While on Pt(111)[4−8] the only surface reaction product is methane, on copper higher hydrocarbons may form as well.[10−13] More reactive metals like Ni[16] and Ru,[3] further dissociate the methyl fragments, which results in surface carbide and gradual desorption of hydrogen.

It is, therefore, worthwhile to study the chemistry of somewhat less reactive methyl halide—CH_3Br, on one of the most reactive methanation surfaces—Ru(001)—with the goal to learn the delicate balance between various reactivity channels in the presence of the bromine atom as a coadsorbate.

In this work we present an investigation of the adsorption, desorption and thermal decomposition of methyl bromide on Ru(001). By monitoring the work function change during adsorption, the dipole moment and polarizability could be extracted, and the nature of interaction of this molecule up to the third layer could be revealed. Using a combination of normal TPD (Δp-TPD) and work function measurements during sample heating ($\Delta\varphi$-TPD), the onset of decomposition at low coverages and the formation of "bulklike" structure at the third

[⊗] Abstract published in *Advance ACS Abstracts,* September 1, 1997.

S1089-5647(97)01134-6 CCC: $14.00

layer and above have been characterized. The dissociation pathways of the methyl fragment as the crystal temperature increases, the effect of deuterium preadsorption, and the coadsorption of bromine atoms are discussed.

II. Experimental Section

The experiments described here were performed in an ultrahigh vacuum (UHV) chamber with a base pressure of 3×10^{-10} Torr obtained by turbomolecular (240 L/s) and titanium sublimation pumps. A sputter gun (Ar^+ ions at 600 V and sample current of 8 μA were typically used) to clean the Ru(001) surface and a quadrupole mass spectrometer (VG, Masstorr DX) for Δp-TPD spectra were used. The QMS was covered by a Pyrex shroud with 0.5 cm diameter aperture. This effectively prevents contributions to the Δp-TPD spectra from surfaces other than the sample. A kelvin probe (Besocke Type-S) was employed to monitor work function change ($\Delta\varphi$) . Both $\Delta\varphi$-TPD and Δp-TPD were measured as a function of crystal temperature using the same routine. A computer controlled ac-resistive heating method could at the same time control the sample heating rate or stabilization temperature ($\pm$0.1 K). The signal is stored via an A/D converter from either the quadrupole to obtain Δp-TPD or from the kelvin probe controller to obtain $\Delta\varphi$-TPD spectra. Differentiating the $\Delta\varphi$-TPD data for desorbing species generates spectra that correspond to normal Δp-TPD.[18] Differences in the peak positions of the two types of TPD modes reveal chemical changes in the adsorbate layer prior to desorption. This is a unique capability of these work function measurements. At typical heating rate of 2 K/s, up to 7 masses, could be monitored simultaneously using the Δp-TPD routine. The quadrupole sensitivity to different masses and the cracking pattern in the ionizer have been taken into consideration when calibrating relative signal intensities at different masses.

The Ru(001) sample (a square piece, 8 × 8 mm, 1.5 mm thick) was cut from a single crystal rod to within $\pm 1°$ of the (001) crystallographic orientation and was polished by diamond paste having particles of 0.25 mm. Sample cleaning in UHV included sputtering for 5 min and then 2 cycles of exposure to 1×10^{-7} Torr of oxygen for 3 min at a crystal temperature of 800 K to remove carbon, followed by flashing to 1630 K, which anneals the sample and removes all oxygen from the surface. LEED from the clean and annealed surface showed very sharp hexagonal patterns. Δp-TPD spectra of CO and N_2, which were identical to results in the literature,[18,19] were used as an additional verification for cleanliness and proper surface structure. The sample was spot welded between two 0.5 mm diameter tantalum wires and was attached to a liquid nitrogen reservoir via copper feedthroughs directly welded to the bottom of the Dewar. By pumping over the liquid nitrogen, a surface temperature of 78 K could be obtained. The temperature was monitored by a W5%Re−W26%Re thermocouple spot welded to the edge of the ruthenium sample.

CH_3Br (99.5% pure) was further purified by a few freeze−pump−thaw cycles to eliminate any noncondensable residual gases. Exposure was done by filling the chamber through a leak valve to the desired pressure, and the ion gauge signal was then transmitted to a computer and converted to langmuir units (1 langmuir = 10^{-6} Torr·sec). Br_2 99.5% pure was evaporated without further cleaning through a 3 mm i.d. doser attached to a leak valve to minimize background pressure increase.

III. Results and Discussion

A. Adsorbed CH_3Br. Temperature-programmed desorption spectra (Δp-TPD) at the molecular mass of 94 amu after exposing the Ru(001) surface at 82 K to increasing amounts of methyl bromide are shown in Figure 1. Desorption peaks are centered at 155 (γ), 160−195 K (γ'), 129 K (β), 119 K (α'), and 126 K (α). The ($\gamma + \gamma'$) and the β peaks are attributed to methyl bromide molecules desorbing from the first and second layers, respectively. The α' and α peaks are observed at higher coverages. The nature of these peaks will be discussed below. The monolayer coverage has been determined to consist of 3.6 ($\pm$ 0.3) × 10^{14} molecules/cm^2, equivalent to $CH_3Br/Ru = 0.22 \pm 0.02$, as will be shown in section D. The density of the crystalline CH_3Br in the (001) plane is 6.96×10^{14} molecules/cm^2, as obtained from X-ray studies.[21] Thus, we conclude that upon completion of the first layer the density reaches 52 ± 5% of its value in the bulk molecular crystal.

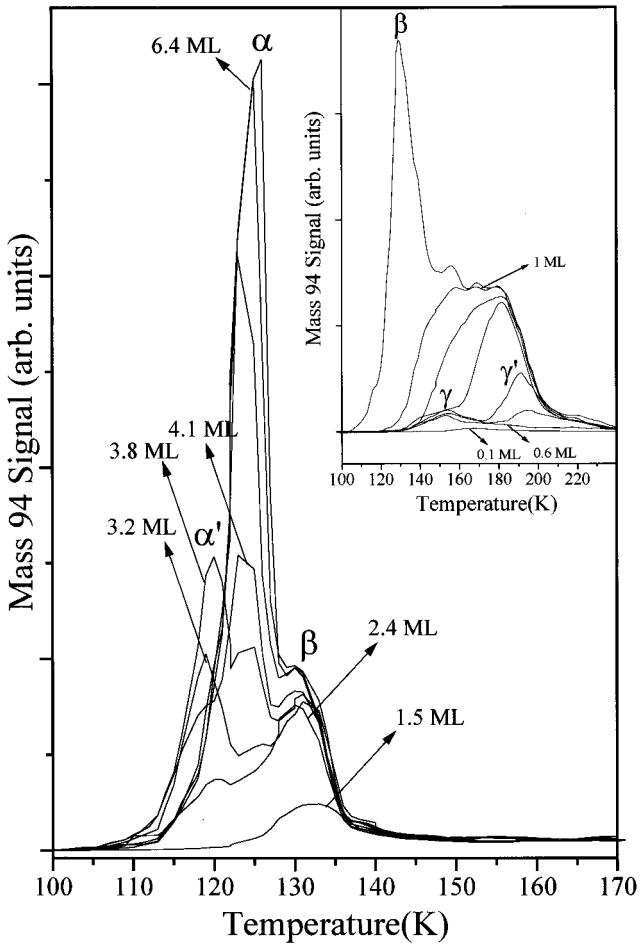

Figure 1. Δp-TPD spectra of CH_3Br from Ru(001) at the indicated coverages (1.5−6.4 ML, 1 ML = (3.6 ± 0.3) ± 10^{14} molecules/cm^2). The adsorption temperature was 82 K and the heating rate 3 K/s. In the inset the coverage range is 0.1−1.5 ML.

Throughout this paper θ signifies the ratio of the number density of molecular methyl bromide to ruthenium atoms (θ = $CH_3Br/Ru = 0.22$ at 1 monolayer (ML), while Θ is used to describe relative numbers in units of monolayers (for $\Theta = 1$ ML, $\theta = 0.22$). The spectra in Figure 1 correspond to coverages (Θ) in the range 1.5−6.4 ML, as indicated. In the inset of Figure 1, Δp-TPD spectra are shown that zoom in on the low-coverage desorption features. Below 0.6 ML less than 6% of the parent molecules desorb molecularly, while the rest dissociate upon crystal temperature increase to form CH_3(ad) and Br(ad). The meaning of the different peak desorption positions as a function of coverage, detected by either Δp-TPD or $\Delta\varphi$-TPD modes, will be discussed below.

The total molecular uptake, obtained by integrating the area under the Δp-TPD peaks, is given in Figure 2. The constant slope of the coverage vs exposure plot, for exposures that result

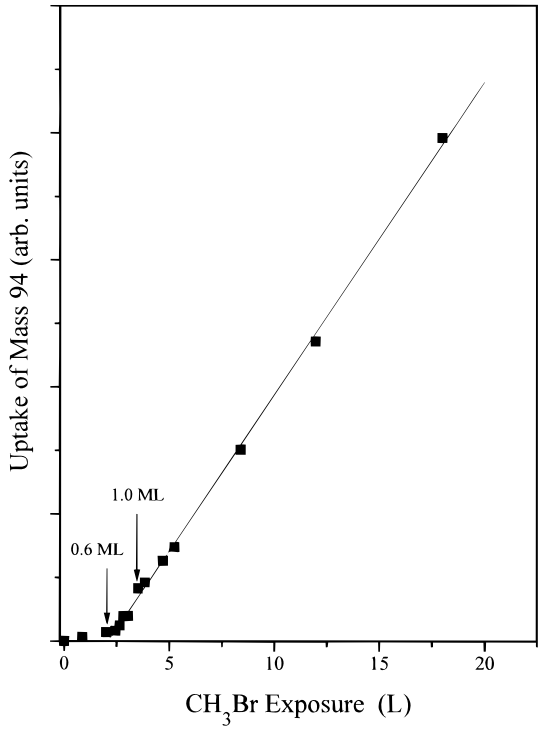

Figure 2. Uptake of CH_3Br desorbing from Ru(001) vs exposure in langmuirs (integrated Δp-TPD spectra at mass 94).

in more than 0.6 ML, indicates that the sticking probability of the molecular methyl bromide is coverage independent. This curve also suggests that there is no significant addition to dissociation from the subsequent molecules above 0.6 ML. This indicates that the reactivity of the clean Ru(001) surface toward dissociation of CH_3Br is poisoned by the first 0.6 ML of dissociating molecules. As has been indicated in other studies of methyl halides on metal and semiconductor surfaces,[3−14,20] the sticking probability of methyl bromide on Ru(001) is assumed to be unity as well.

Information on the dipole moment and polarizability of the adsorbed methyl bromide prior to any sample heating (as occurs in TPD) can be obtained by measuring the work function change during CH_3Br adsorption. We found that 1 monolayer of the methyl bromide corresponds to an exposure of 3.5 langmuirs (uncorrected ion gauge signal).

In Figure 3 $\Delta\varphi$ is measured while the Ru(001) surface at 82 K is exposed to CH_3Br. The exposure range necessary to populate the various desorption peaks, as found from the integrated Δp-TPD spectra after the corresponding CH_3Br exposures, is indicated. The first layer completes slightly after the minimum in the work function vs exposure curve (3.5 langmuirs), while the second-layer population starts slightly before the minimum in the work function curve is reached. This indicates that the first 0.9 ML adsorbs exclusively at the first layer and at coverages approaching 1 ML both the first and second layer are populated simultaneously. Similar conclusions were reached in the study of the CH_3I/Pt(111) and CH_3Br/Pt(111) systems,[7,8] where only above 0.9 ML has the population onset of the second layer been recorded by RAIRS. Practically identical results were obtained also for CH_3Cl on Pd(100).[22]

The work function *decreases* by 2.15 V upon completion of the first layer. This large work function change suggests that the molecule adsorbs with the bromine atom pointing toward the surface. Molecules in the second layer lead to *increase* of the work function. This indicates that the majority of these molecules adsorb in a different geometry than the molecules in the first layer and probably with the methyl pointing toward

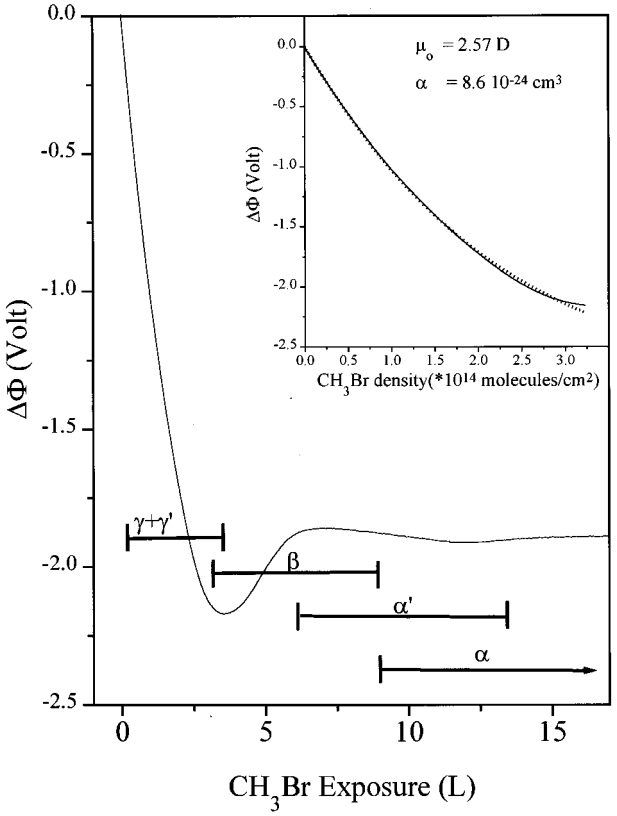

Figure 3. Work function measurement during adsorption of CH_3Br on Ru(001) at 82 K. The onset and completion of each of the layers are indicated. In the inset the fit of the data (solid line) to the MC model (dotted line) is shown . The isolated molecule dipole moment and polarizability are derived from this model (see text).

the surface. The exact value of $\Delta\varphi$ that pertains to the second-layer molecules is difficult to assign due to simultaneous adsorption of second and higher layers. A lower limit *increase* is estimated at 350 mV. Molecules in the third and higher layers adsorb following exposure of 13.3 langmuirs contribute a small *negative* change of work function of approximately 80 mV. This is a significant contribution taking into account how far these molecules are from the surface. Further exposing the surface to more than 13.3 langmuirs results in further small work function increase. This increase might be due to induced rearrangement of molecules already adsorbed in the third layer to a configuration that mimics the bulk structure of alternating molecular geometry.[21] Eventually, when the bulk structure is formed no further change in the work function is expected.

Analysis of work function vs adsorption curves employing the Topping equation provides information on the adsorbates' dipole moment and polarizability.[23] The effects of immobile adsorbates and coadsorbates on the measured work function change were studied using a similar approach[24,25] and have also been extended to the analysis of Δp-TPD spectra.[26,27] The effect of dipole−dipole interactions on the observed Δp-TPD as a function of coverage has recently been refined to include image dipole effects for cases of strong metal−adsorbate interactions by Maschoff and Cowin (MC model).[28] Extraction of dipole moment and polarizability from Δp-TPD spectra were demonstrated for alkyl halides in cases where no dissociation takes place, e.g. CH_3Cl on Pd(100)[22] and CH_3X (X = Cl, Br, I) on GaAs(110),[20] without inclusion of the image dipoles' effects. The application of the MC model was recently demonstrated for the CH_3Cl/Cu(110) system.[27]

Studying the interaction among neighbor adsorbates via thermal desorption data as has been done for CH_3Cl on

Cu(110) is impossible where partial dissociation occurs during Δ*p*-TPD, as is the case in the CH_3Br/Ru(001) system. We can, however, analyze the work function change measured during adsorption when it is recorded at a crystal temperature of 82 K, since no dissociation takes place at this temperature (details in section C, below).

Assuming free mobility of the CH_3Br adsorbates on the surface at 82 K to produce a uniform distribution on the hexagonal Ru(001) surface, we employ the MC model mentioned above to evaluate the dipole moment of the adsorbates as a function of coverage.[28] Dipole length d (separation between charges) and center of the dipole to image plane distance β, are the primary parameters of this model. As in the Topping model,[23] the potential energy for an adsorbed dipole that results from electrostatic interaction with other dipoles in a two-dimensional array of density n is calculated. Stabilization energy due to the interaction of the dipole with the screening image charge induced on the metal surface, which was neglected in the Topping model, is included.

The work function change $\Delta\varphi$ is thus given by[28]

$$\Delta\varphi = -\frac{4\pi\mu_0 n}{1+\alpha\left(F(n)-\frac{1}{4\beta^3-\beta d^2}\right)} \qquad \mu_0 > 0 \quad (1)$$

where

$$F(n) = \frac{4\pi}{\sqrt{3}CR_s^3}\left(1+\frac{1}{\left[1+\left(\frac{2\beta}{CR_s}\right)^2\right]^{3/2}}\right) \qquad (2)$$

$F(n)$ depends on the surface geometry and describes the characteristics of the electric field due to neighbor dipoles where

$$R_s = \frac{(4/3)^{1/4}}{n^{1/2}} \qquad C = 0.658 \qquad (3)$$

n is the surface density of methyl bromide molecules, μ_0 is the dipole moment of an isolated adsorbate in the absence of image dipole stabilization,[28] and α is its polarizability.

The C−Br bond distance in the crystalline CH_3Br is 1.86 Å as obtained from X-ray studies.[21] Taking the van der Waals radius of the Br atom to be 1.95 Å,[29] we set $\beta = 2.85$ Å and $d = 1.86$ Å as fixed parameters. Additionally, we define $n_s = 3.6 \times 10^{14}$ molecules/cm^2 to be the density of 1 ML of methyl bromide molecules on the Ru(001) surface, based on calibration of CH_3Br coverage that will be discussed in section D.

Fitting the work function data requires adjustment of two free parameters, μ_0 and α. The inset of Figure 3 shows the fit of the calculated (dotted line) work function change (eq 1) to the experimental data (solid line) with $\mu_0 = 2.57$ D (1 D = 3.34×10^{-30} C·m) and $\alpha = 8.6 \times 10^{-24}$ cm^3 as the best fit parameters. These numbers are larger than the corresponding gas phase values of 1.81 D and 5.57×10^{-24} cm^3.[28] At higher coverages ($\Theta > 0.9$), the experimental points slightly deviate from the line predicted by eq 1. Positive contribution to $\Delta\varphi$ due to the simultaneous partial adsorption at the second layer can lead to this effect. In addition, molecules that adsorb with the methyl group pointing toward the surface, which are expected at the highest coverages (see discussion below), will affect the work function in the same way. Positive deviation may also arise from minor coverage dependence in α. Both the dipole moment of the isolated molecule and the polarizability are larger than the corresponding gas phase values. This reflects the strong interaction of methyl bromide with ruthenium, which correlates well with the reactivity of this surface toward dissociation.

From our work function data we cannot definitely conclude whether the methyl bromide molecules adsorb vertically or are tilted with respect to the surface normal at coverages below a monolayer. A tilted adsorption geometry was concluded in the case of CH_3Br and CH_3I on Pt(111).[6−8] However, the large dipole moment measured at low coverages strongly supports the prediction that it is adsorbed vertically with the bromine down on Ru(001). Any tilt by an angle ϕ from the surface normal results in an increase of μ_0 by a factor of $\cos(\phi)^{-1}$, making it a rather unphysical value.

The large dipole moment at low coverages excludes the possibility that at 82 K the methyl bromide molecules dissociate upon adsorption. We reach this conclusion because the separate work function contribution of the methyl and the bromine fragments is far smaller than the molecular one (details in section C, below).

B. Δ*p*-TPD and Δφ-TPD: $\Theta < 0.6$ ML. At coverages below a monolayer of CH_3Br, two main competing reaction channels simultaneously take place during sample heating in the temperature range of 82−200 K: dissociation to CH_3(ad) and Br(ad) and molecular desorption. A minor third reaction channel is methane production and immediate desorption. Unlike the case of CH_3I /Ru(001),[3] where methane production is an important channel, here this route is effectively blocked in the above temperature range. The branching between these channels changes gradually with coverage. Dissociation dominates at $\Theta < 0.6$ with hardly any desorption, while above this coverage molecular desorption becomes the faster and dominant channel. The change in the branching discussed above is clarified in Figure 2, where the total Δ*p*-TPD uptake of the molecular desorption (at mass 94) is presented. The extent of dissociation of the parent molecules is determined by the amount of adsorbed hydrogen, which results from further decomposition of adsorbed methyl on the ruthenium surface; see the discussion below.

A significant and sudden change in the molecular Δ*p*-TPD is found for coverages $\Theta > 0.6$. A new site is populated, characterized by a peak desorption at 195 K (γ'), which is higher by 40 K from that observed at lower coverages, near 155 K(γ). This is shown in the inset of Figure 1. Population of more strongly bound sites at *higher* coverages is rather unusual due to repulsion between neighbors expected at higher densities. This higher peak temperature gradually shifts back to lower temperatures as coverage further increases. The shift to lower temperatures observed for $0.6 < \Theta < 1$ can be explained in terms of dipole−dipole repulsions.[28]

Examination of the work function change measured during adsorption at 82 K (Figure 3) does not clarify the origin of the new molecular adsorption site desorbing at 195 K. There is no break or sudden change in the work function near or above 0.6 ML adsorption. This implies that the new site observed above 0.6 ML is formed by the coadsorption of CH_3Br and its fragments as a result of the partial dissociation that occurred during the TPD process. In this temperature range most of the fragments are CH_3 (ad) and Br(ad). We were led to this conclusion by the following arguments:

(a) Comparison with Δ*p*-TPD of CH_3Cl,[30] which does not dissociate on Ru(001) in the same temperature range and does not show this unusual behavior. (b) Upon partial passivation of the ruthenium surface by deuterium preadsorption, which slows down the dissociation channel of CH_3Br, the intensity of this high-temperature desorption peak is reduced. It is not clear, however, what exactly is the nature of the attractive interaction

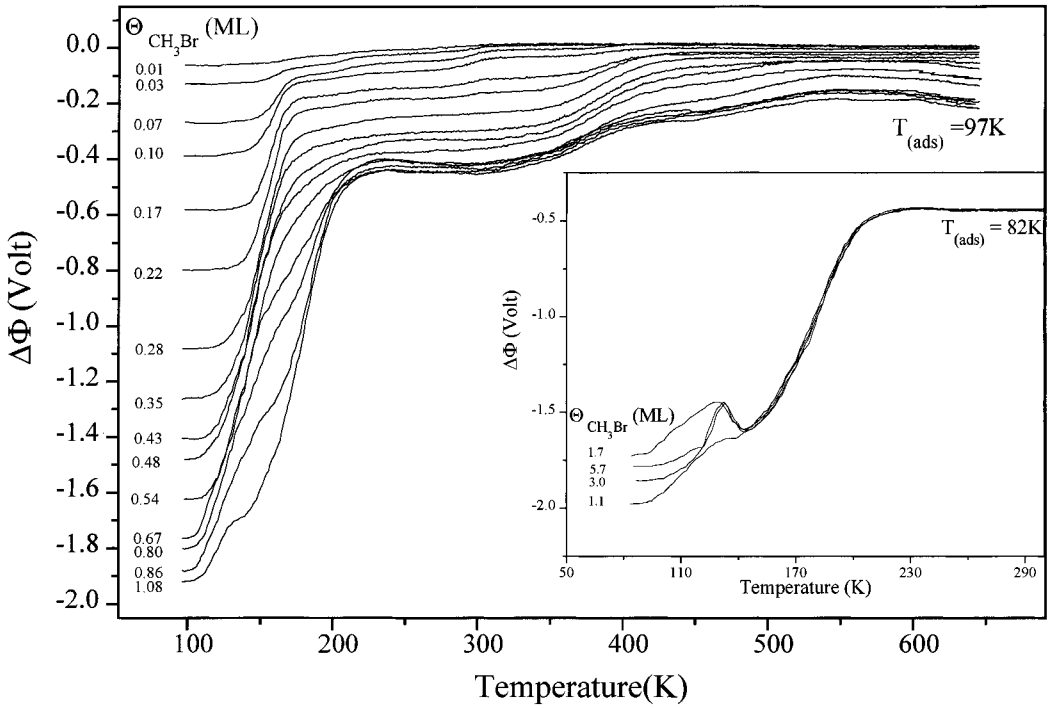

Figure 4. Work function change during temperature-programmed desorption ($\Delta\varphi$-TPD) of the first layer of CH_3Br from Ru(001) at the indicated initial coverages. The adsorption temperature was 97 K and the heating rate 2 K/s. In the inset $\Delta\varphi$-TPD spectra are shown for coverages above 1 ML, at an adsorption temperature of 82 K.

between CH_3Br and either CH_3(ad) or Br(ad), which increases the binding energy by almost 10 kJ/mol. On most surfaces, adsorbed halides will induce a work function increase.[31−33] In such a case one could explain this shift on the basis of electrostatics: attraction between opposite dipoles (CH_3Br and Br). However, as will be discussed in section E, bromine atoms adsorbed on the Ru(001) surface unexpectedly decrease the work function, thus excluding simple electrostatics as a basis for this attraction. It may, therefore, result from more complex, yet unclear, interaction that involves the parent molecule and the methyl fragment.

Information on surface processes that occur at coverages and temperatures below the onset of desorption can be obtained from $\Delta\varphi$-TPD spectra. In Figure 4 a set of such spectra at different initial methyl bromide coverages is shown. Change in work function during sample heating precedes desorption, in particular at low coverages where dissociation is the dominant channel. This is clearly illustrated by differentiating the $\Delta\varphi$-TPD spectra with respect to temperature, as presented in Figure 5a for coverages between 0.07 and 1 ML. The peaks obtained at coverages where molecular desorption is a minor channel of reactivity ($\Theta < 0.6$) necessarily arise from other surface processes. At the lowest coverages these peaks directly correlate with molecular decomposition near 125 K. Contribution to $\Delta\varphi$ from molecular desorption at these coverages is estimated to be less than 10% of the total observed $\Delta\varphi$ values. This unique feature of the $\Delta\varphi$-TPD mode, where surface processes other than desorption are directly monitored, identified, and characterized, is of great importance in the study of reactive adsorbate−metal systems.

At coverages approaching a full monolayer, a shift of the $d(\Delta\varphi)/dT$ signal to lower temperature is observed, while the desorption peak of the parent molecules stays practically unchanged at the low-temperature desorption edge. Δp-TPD performed at these high coverages at mass 16 revealed a small peak believed to originate from methane production at temperatures below 120 K. The methane (full lines) and methyl bromide (dashed lines) Δp-TPD spectra are shown in Figure 5b.

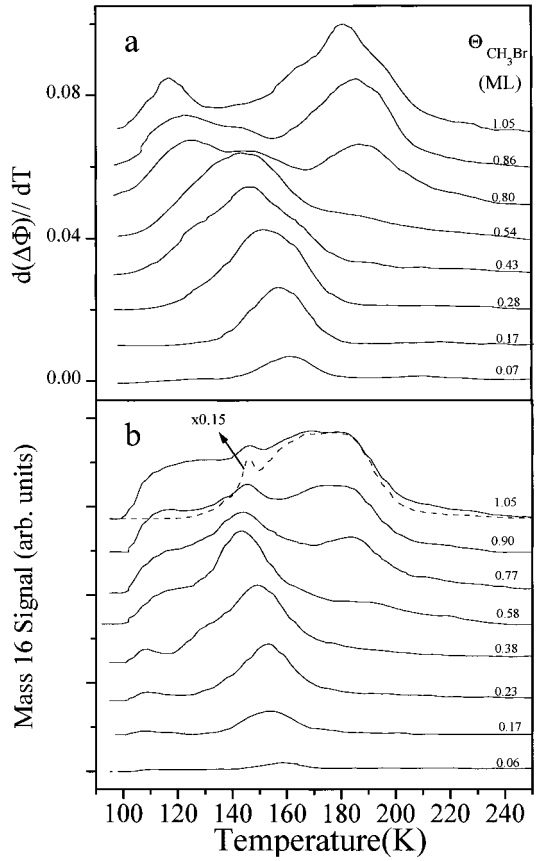

Figure 5. (a) Differential $\Delta\varphi$-TPD spectra ($d(\Delta\varphi)/dT$) for the indicated initial coverages of CH_3Br. The adsorption temperature was 97 K and the heating rate 2 K/s. (b) Δp-TPD of CH_4 (mass 16, solid line). The adsorption temperature was 97 K and the heating rate 3 K/s. For comparison a Δp-TPD spectrum of CH_3 Br (mass 94) is shown as a dashed line at a coverage of 1.05 ML.

Below 120 K, a change in the work function cannot be due to desorption of parent molecules. We have excluded the pos-

sibility of methane production in the QMS ionizer. This was done by preexposing the surface to deuterium, which produces CH_3D (mass 17) at the same low temperatures and therefore rules out possible contribution from the ionizer of the QMS (expected to contribute only at mass 16). Another check of the fact that production of methane is only at the surface was done by passivation of the Ru surface by evaporating 2 ML of Cu on it. On this Cu/Ru(001) surface CH_3Br does not dissociate and indeed, as expected, no methane is produced below 120 K.[34]

One should consider the possible involvement of defects in the production of methane described above. Defects are typically known to be decorated at the lowest coverages due to their higher binding energy and therefore are expected to be covered by parent molecules and fragments while surface heating takes place. However, as shown in Figures 4 and 5, both the work function change and methane production are negligible in the low-coverage regime. It is unlikely, therefore, to have the methane production at steps and other defects taking place only as the coverage increases.

Two phenomena observed at $T_s < 120$ K (see Figure 5) need to be explained:

1. The work function increases with concomitant desorption of small number of methane molecules prior to the parent molecule's desorption onset.

2. The onset for work function increase shifts to lower temperatures as coverage increases, down to less than 82 K near a monolayer. Two possible explanations are discussed below: the dissociation of parent molecules and molecular restructuring.

b.1. Molecular Dissociation. The concomitant work function increase and desorption of small amount of methane at temperatures prior to molecular desorption could in principle be rationalized by the dissociation of methyl bromide to its methyl and bromine fragments before desorption. Such dissociation would increase the work function due to the far smaller dipoles of the separate adsorbed fragments compared to the parent methyl bromide molecule. However, thermal decomposition is not expected to shift to lower temperatures as coverage increases as long as it adsorbed with the bromine toward the surface. In fact, the opposite is predicted because the C−Br bond energy should increase somewhat with coverage. This can be understood via the strong dipole−dipole repulsion among neighbors, which slightly decreases the binding energy of the molecule to the metal (through the Br−metal bond), as indicated by the shift of the desorption onset to lower temperatures as coverage increases; see Figure 1. Weakening the bromine−metal bond should lead to strengthening of the intramolecular carbon−bromine bond.

Another dissociation route that can be considered is the thermally activated dissociative electron attachment (DEA) scheme, which has been suggested to explain the results of the CH_3I/Cu(111) system.[35] Thermal electron excitation from the Fermi level, followed by attachment to the adsorbed molecule, creates a transient negatively charged excited molecular adsorbate. This anion may then deexcite while decomposing. A mechanism of this kind strongly depends on the work function of the system, and its probability should scale with the extent of work function decrease in the system upon adsorption. The DEA process should lead to work function increase (similar to the simple thermal decomposition), but in addition an ejection of the methyl group during the DEA process (which has been reported to occur in the CH_3I/Cu(111) system[35]), if it occurs, would result in additional increase of the work function. In our system, no ejection of methyl radicals to the gas phase was found.

The same arguments, however, used to exclude the low-temperature thermal dissociation channel should be applied here as well: Molecular dipole moments are largest at low coverages, where depolarization effects due to dipole−dipole repulsions can be neglected. As a result, the *local work function* at the vicinity of the adsorbate should increase with coverage; therefore, the probability for the DEA process should decrease. This excludes the DEA scheme as an explanation of the observed increase in the work function upon heating and to the shift of the $d(\Delta\varphi)/dT$ signal to lower temperatures with coverage. Finally, none of the above decomposition models can explain the minor low-temperature production and desorption of methane.

We conclude that low-temperature ($T_s < 120$ K) dissociation schemes of the parent molecule are less likely to explain the observations in this temperature range.

b.2. Molecular Restructuring. We now consider a thermally activated process in which the dipole−dipole repulsion that strongly affects nearest CH_3Br neighbor molecules forces one from each pair of neighbor adsorbates to flip over. This would result in the formation of antiparallel adsorption pairs, which should significantly reduce the destabilizing repulsion energy between neighbors on the surface. Such packing of molecules, with opposing adjacent dipoles, is the preferred geometry found in the molecular crystal of methyl bromide, as revealed by X-ray studies.[21] From Figure 5a we see that the onset for the increase in work function gradually shifts from 140 K at 0.07 ML to 100 K at 0.54 ML. At coverages approaching 1 ML ($\theta = 0.22$), this onset shifts to temperatures lower than 82 K .

On the basis of the discussion above, we consider the possibility that the increase of work function at temperatures below 120 K arises from thermally activated restructuring of parent molecules into the molecular crystalline geometry.[21] If indeed a fraction of the adsorbed molecules flip over to the "methyl down" configuration, it may explain the observed work function increase. This may result in a simultaneous decomposition of a small fraction of these molecules due to the increased reactivity of the Ru(001) surface toward this configuration, which is forced on the molecules due to the strong dipole−dipole repulsion among adjacent molecules. It is thus proposed that once a methyl group is formed at this temperature range, surrounded by parent molecules and some residual surface hydrogen, it immediately recombines to desorb as molecular methane. The relevant fraction of desorbing methane molecules at $\theta = 0.22$ below 120 K is 4% of the parent molecules. From this number we conclude that most of the flipped over molecules with the methyl down configuration are stable on the surface below 120 K. The majority of the methyl fragments eventually formed by the dissociating parent molecules are stable on the surface up to 210 K, as will be discussed below.

An interesting case of flipping over an adsorbed molecule when it resides next to an adsorbed alkali metal due to its strong local electric field has been shown for water on K/Pt(111) and K/Ru(001).[36−38] In analogy to these examples, the effective local electrostatic field generated by an adsorbed methyl bromide increases with coverage since the average distance between neighbors decreases. The repulsion energy is expected to depend roughly on $1/r^3$, r being the average distance between neighbor adsorbates. For a homogeneous distribution of adsorbates this interaction energy will increase with coverage as $\theta^{3/2}$. However, unlike the water−alkali metal case, thermal activation for flipping the molecule is necessary in the CH_3Br/Ru(001) system. Only at coverages approaching 1 ML is such flipping possible already upon adsorption at 82 K, as discussed

above. This is consistent with the smaller dipole of methyl bromide compared with that of alkali metals.

A quantitative analysis to check the validity of the somewhat speculative electrostatic flipping model is currently beyond the signal to noise level of our work function data. However, our results clearly show that the leading edge of the $d(\Delta\varphi)/dT$ spectra (Figure 5) shifts to lower temperatures as coverage increases. This qualitatively correlates with a decreasing apparent activation energy for flipping, an analysis that is a standard in the discussion of Δp-TPD data.

A third possibility to explain the low-temperature increase in work function is a thermally activated rearrangement of the parent molecules into different sites, orientation, or layer. CH_3Br on Pt(111) was found to adsorb exclusively at the on-top sites at coverages up to $\theta = 0.10$ (adsorption temperature of 20 K, than brief annealing to 90 K), and only at higher coverages do other sites become populated.[8] Assuming different dipole moments at the various adsorption sites also in our system, we anticipate a break in the adsorption work function curve, shown in Figure 3, around the saturation of the on-top site. The smooth decrease observed in the work function curve is inconsistent with such a population scheme.

CH_3Br is known to adsorb via the bromine atom on most transition metal surfaces at coverages of a monolayer or less.[17] On Ru(001) the *decrease* of 2.15 V in work function is consistent with the same geometry. The dipole moment of the isolated adsorbed molecule excluding image dipole effects is found to be 2.57 D (see work function analysis above). This is larger than the gas phase value of 1.81 D. It suggests that the molecule is bound with its axis normal to the surface with no significant tilt even at the lowest coverages. Time-of-flight analysis of the methyl group following photodissociation of CH_3Br on Ni(111)[16] and CD_3I on TiO_2[39] have indicated that perpendicular adsorption geometry is consistent with the results for submonolayer coverages. CH_3I on Pt(111)[7] and on GaAs(110),[20] on the other hand, are reported to adsorb with its C−I bond axis tilted at 45° with respect to the normal to the surface, with decreasing tilt (18°) at 1 ML.[7] Even if CH_3Br is tilted also on Ru(001) with decreasing tilt angle as coverage increases, its effect on the work function is predicted to be opposite to the observed trend.

A decrease in the density of the first layer by thermally activated 3D cluster formation can be yet another possible explanation. However, the IRAS measurements mentioned above of CH_3Br on Pt(111)[8] indicates that upon annealing the surface to temperatures exceeding that of multilayer desorption, no evidence for 3D formation is observed.

To summarize this section, with the quality of data currently available, we are unable to unambiguously conclude what is the mechanism that causes the low-temperature work function increase preceding desorption that shifts to lower temperatures as coverage increases. We tend to favor the flipping mechanism, which seems to be most consistent with the experimental data, but, needs to be quantitatively verified in the future.

C. Decomposition of the Methyl Fragment: $\Theta < 0.6$ ML. The predominant channel of reactivity at methyl bromide coverages below 0.6 ML leads to dissociation to form CH_3(ad) and Br(ad) after heating the surface above 125 K. The methyl fragment undergoes further decomposition as the crystal temperature is raised. The chemistry of adsorbed methyl in the presence of iodine has been investigated for the case of CH_3I decomposition on Ru(001) employing HREELS and TPD.[3] Hydrogen atoms accumulated on the surface during the decomposition of CH_3(ad) recombine and desorb as H_2 only above 260 K; therefore, its Δp-TPD cannot be used to monitor the onset of each step of the decomposition process. The $\Delta\varphi$-TPD method, on the other hand, reveals clear changes in the work function while heating the sample at temperatures below hydrogen desorption and therefore can be used to directly follow each of the decomposition steps.

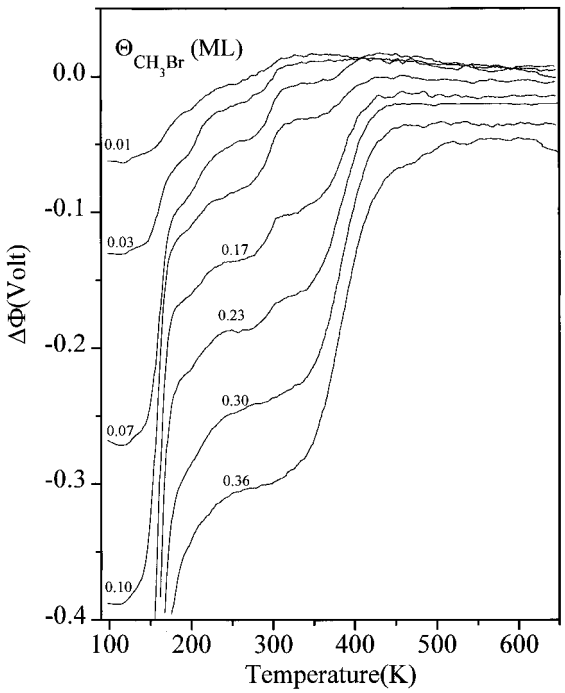

Figure 6. $\Delta\varphi$-TPD in the low-coverage regime of CH_3Br. The adsorption temperature was 97 K and the heating rate 2 K/s.

In Figure 6 $\Delta\varphi$ is recorded as a function of crystal temperature for different low initial coverages of the parent molecule. As mentioned above, the major initial increase of $\Delta\varphi$ above 130 K for $\Theta < 0.6$ follows the parent molecules' dissociation (desorption becomes the dominant process affecting $\Delta\varphi$ at higher coverages). If we focus our attention to changes in work function at temperatures above 200 K, molecular desorption should not contribute to the $\Delta\varphi$ signal. Only methyl fragment's chemistry should thus be relevant. An increase in the work function is clearly observed near 210, 290, 320, and 380 K. Around 450−600 K additional but smaller changes in $\Delta\varphi$ are observed. These changes in the slope of the work function vs temperature curves can be emphasized by differentiating the $\Delta\varphi$-TPD spectra. In Figure 7 a set of such spectra for $T_s >$ 190 K is presented (solid lines), and the various peaks are marked as $\alpha_1-\alpha_3$ and $\beta_1-\beta_4$ for coverages below and above 0.35 ML, respectively. Together with the $d(\Delta\varphi)/dT$ spectra, the corresponding hydrogen Δp-TPD spectra (dotted lines) are presented. For comparison, the Δp-TPD spectrum of hydrogen produced from the clean Ru(001) surface at 0.33 ML (dashed line) is shown as well. This is the hydrogen uptake expected following the thermal decomposition of 1 ML of methyl bromide, where 1 ML is defined as H/Ru(001) = 1.[40]

At temperatures above 200 K new decomposition pathways are observed. The $\Delta\varphi$ rise at 210 K in Figure 6, partially shadowed by the molecular desorption effect on the work function at high coverages, originates from the dissociation of CH_3(ad) to CH_2(ad) + H(ad). This change in the work function is particularly significant in the α_1 peak, see Figure 7. Heating the surface beyond 230 K reveals a gradual change in the dissociation pathway while increasing the initial coverage. This is shown in Figure 7, where a peak at 290 K (α_2) gradually increases with coverage and disappears around 0.35 ML. We attribute this peak to the dehydrogenation of CH_2(ad) to CH-

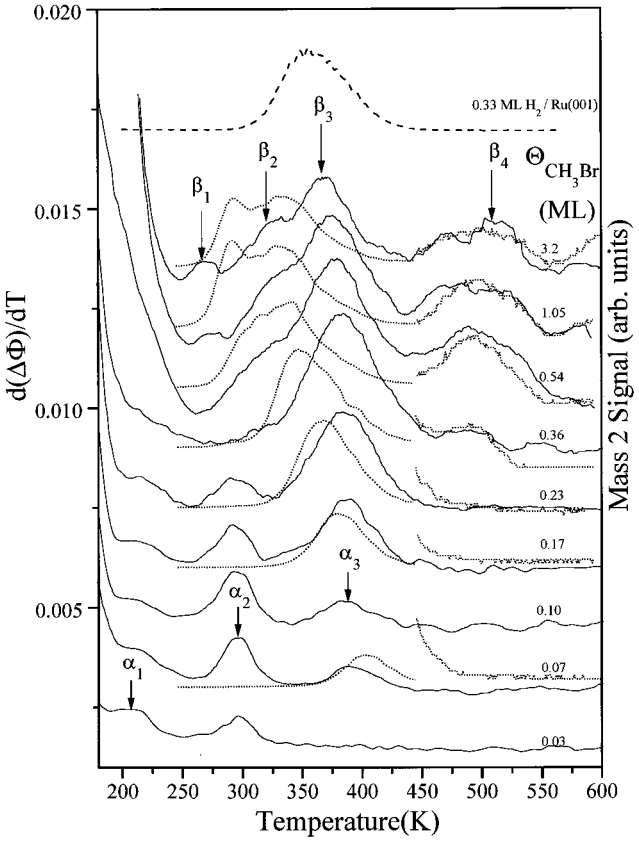

Figure 7. Differential $\Delta\varphi$-TPD spectra ($d(\Delta\varphi)/dT$) after the decomposition of CH_3Br to CH_3(ad) + Br(ad) has been completed (solid line), together with the corresponding hydrogen Δp-TPD spectra (dotted line) for the indicated initial coverages in monolayers. The hydrogen Δp-TPD spectra for temperatures exceeding 450 K are 10-fold magnified. Δp-TPD of 0.33 ML of hydrogen from the clean Ru(001) surface is presented as a reference (dashed line at the top).

(ad) + H(ad). Similar behavior was observed in the HREELS study of CH_3I on Ru(001),[3] where CH_2(ad) was shown to decompose near 280 K. At coverages higher then 0.35 ML the 280 K peak disappears and a new one (β_1) emerges at 270 K. Disproportionation of two CH_2 (ad) fragments to ethylidyne (CCH_3 (ad)) has been proposed[3] to occur near 280 K at the high-coverage regime. At this temperature, the hydrogen recombinative desorption Δp-TPD peak is observed as well. The second-order reaction between two methylene fragments becomes the faster reaction in the higher (>0.35 ML) coverage regime. The hydrogen Δp-TPD peak at 280 K does not shift to lower temperatures as coverage increases, a behavior characteristic of second-order reaction, nor does the β_1 ethylidyne formation peak in the $d(\Delta\varphi)/dT$ spectrum. The overlap of these two peaks and their similar coverage independence imply that the hydrogen is generated from the same disproportionation that forms the ethylidyne. This can be rationalized if the ethylidyne formation is rate limited by the CH_2(ad) decomposition.

Ethylidyne was found to dissociate in the temperature range of 290 K−330 K on the clean Ru(001) surface.[41−43] One of the major dissociation products is methylidyne (CCH).[42,43] Unlike the chemistry of C_2H_4 on Ru(001), where ethylidyne is produced from a series of consecutive unimolecular intermediate decompositions,[42−44] in the case of CH_3Br the ethylidyne formation depends upon the encounter probability between two C_1 species (CH_2(ad)). Indeed, a coverage dependence in the ethylidyne formation can be seen in the $d(\Delta\varphi)/dT$ spectra by the appearance of a peak at 320 K (β_2) at coverages higher than 0.35 ML, attributed to the ethylidyne decomposition. Additional support for the suggestion that ethylidyne decomposition is seen only at high coverages is the fact that the high-temperature Δp-TPD peak of hydrogen, believed to arise from ethylidyne decomposition, does not shift to lower temperature above 0.5 ML and stabilizes near 320 K. At lower coverages (up to 0.35 ML), this peak is populated by hydrogen atoms originated from dehydrogenation reactions at lower temperatures and the shift of the peak is due mostly to ordinary second-order reaction kinetics.

A higher temperature peak near 385 K is observed in the $d(\Delta\varphi)/dT$ spectra at coverages above 0.03 ML in Figure 7 and shifts to 370 K at 1 ML. Up to 0.23 ML, hydrogen Δp-TPD demonstrates that no reaction control desorption is seen at $T >$ 450 K. Since the production of ethylidyne is negligible at low coverages, we attribute this peak to dehydrogenation of CH(ad) to C(ad) + $^1/_2H_2$. The shift toward lower temperatures of the CH(ad) dissociation with increasing coverage has been already observed by Hills et al.[42] At increasing coverages another dissociation pathway becomes the dominant one: CCH (ad) → CH(ad) + C(ad) as observed at the temperature range of 350 K−450 K by TPSSIMS[43] and HREELS.[42,43] The fact that the hydrogen desorption temperature is always lower than the $d(\Delta\varphi)/dT$ peak near 380 K at higher coverages indicates that the $\Delta\varphi$ observed is due to surface reaction in which no hydrogen is produced. The hydrogen desorption in that temperature regime is due to the surface crowding and to the expected desorption rate of hydrogen atoms produced at lower temperatures. Thus we attribute the peak in $d(\Delta\varphi)/dT$ around 380 K to dehydrogenation of CH(ad) to C(ad) + $^1/_2H_2$ at low coverages (up to 0.35 ML) and marked as α_3. At high coverages the peak is attributed to CCH (ad) → CH (ad) + C (ad) and marked as β_3. Obviously, we expect the transition between the two regimes to be gradual. The large amplitude in the $d(\Delta\varphi)/dT$ peak at 380 K can be explained by the significant dipole moment change anticipated by the decomposition of CCH(ad) to C(ad) + CH(ad).

At 450 K the only fragments left on the surface at low coverages are carbon atoms, and at coverages higher than 0.35 ML CH(ad) can be coadsorbed with carbon. The broad $d(\Delta\varphi)/dT$ peak centered at 510 K (β_4) is attributed to the dissociation of CH(ad) to C(ad) + $^1/_2H_2$ (g).[41−44] The overlap of the work function peak with that of the (weak) hydrogen Δp-TPD signal supports this assignment.

To conclude the above discussion the following reaction schemes are proposed:

$$CH_3Br(ad) \rightarrow CH_3(ad) + Br(ad) \qquad 125-200\ K$$

$$CH_3(ad) \rightarrow CH_2(ad) + H(ad) \qquad 200-220\ K$$

low coverage ($\Theta < 0.35$)

$$CH_2(ad) \rightarrow CH(ad) + H(ad) \qquad 280-320\ K$$

$$CH(ad) \rightarrow C(ad) + H(ad) \qquad 350-450\ K$$

$$2H(ad) \rightarrow H_2(g) \qquad 320-450\ K$$

high coverage ($\Theta > 0.35$)

$$2CH_2(ad) \rightarrow CCH_3(ad) + H(ad) \qquad 250-290\ K$$

$$CCH_3(ad) \rightarrow CCH(ad) + H_2(g) \qquad 290-340\ K$$

$$CCH(ad) \rightarrow CH(ad) + C(ad) \qquad 340-450\ K$$

$$2H(ad) \rightarrow H_2(g) \qquad 320-450\ K$$

$$CH(ad) \rightarrow C(ad) + {}^1/_2H_2(g) \qquad 450-700\ K$$

At CH_3Br coverages lower then 0.07 ML, no work function change was observed above 450 K while heating the sample

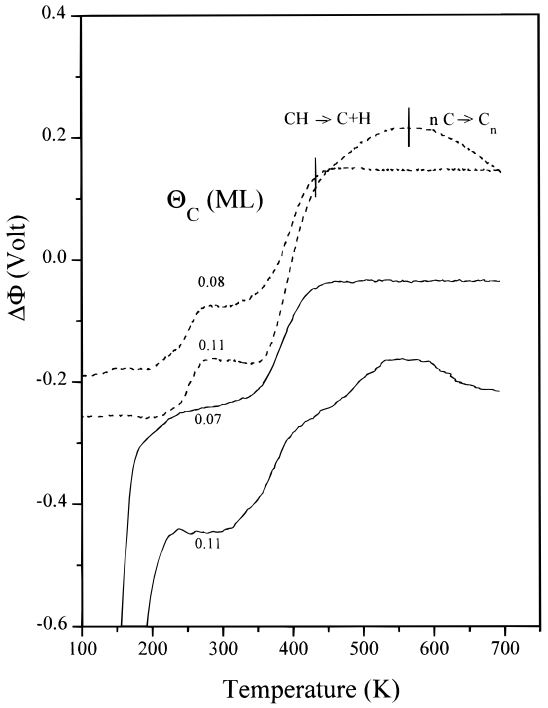

Figure 8. $\Delta\varphi$-TPD spectra of CH_3Br (solid line) and C_2H_4 (dashed line) from Ru(001). The onset of residual carbon polymerization (a maximum in work function near 550 K) is found at carbon coverages between 0.08 ML−0.11 ML in both different systems.

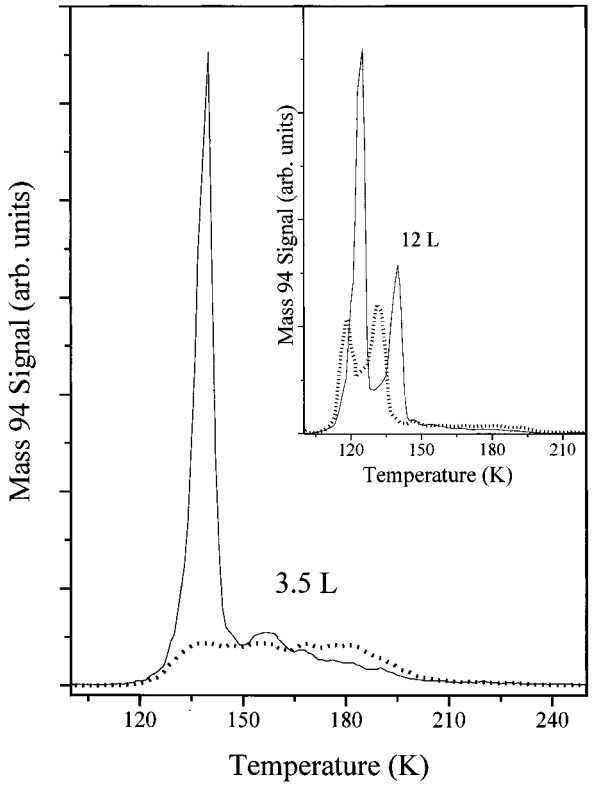

Figure 9. Δp-TPD spectra of CH_3Br following exposure of 3.5 langmuirs on the clean Ru(001) surface (dotted line) and on 0.9 ML deuterium-preadsorbed Ru(001) surface (solid line). In the inset the same Δp-TPD is shown for 12 langmuirs exposure.

covered with a mix of carbide and bromine adatoms. Increasing the initial coverage causes $\Delta\varphi$ to increase up to 530 K followed by a decrease from 560 K. Similar observation has been recorded during $\Delta\varphi$-TPD of C_2H_4/Ru(001),[44] where the same carbide coverage is left on the surface but without coadsorbed halide. These results are summarized in Figure 8 were the $\Delta\varphi$-TPD of C_2H_4 and CH_3Br are illustrated with dashed and solid lines respectively at the indicated carbon/Ru(001) relative coverage. As discussed elsewhere,[45] the temperature onset of carbon polymerization coincides with the decrease in $\Delta\varphi$ near 560 K. This polymerization is very sensitive to the carbon coverage and cannot be observed below 0.08 ML of carbon, consistent with the previous study.[45] The identical minimum carbide coverage that triggers polymerization found in both CH_3Br and C_2H_4 systems indicates that the bromine atoms do not significantly perturb the methylidyne (CH(ad)) decomposition pathway nor the carbide polymerization. However, it is clear from Figure 8 that the work function of the surface covered with the mixed bromide−carbide overlayer is 0.3 V lower than that of the carbide-covered surface. This indicates that bromine decreases the work function, a rather unusual phenomenon with respect to adsorbed halides, which will be verified below following the discussion of results of Br_2 adsorption.

In conclusion, the reactivity channels discussed here demonstrate the strength of work function measurements in the $\Delta\varphi$-TPD mode and their derivative spectra, in providing the exact range of crystal temperature where surface reactions of nondesorbing fragments take place. Comparison of our results to the HREELS study of CH_3I chemistry on Ru(001)[3] shows that the data obtained is complementary. While information from HREELS is species specific, $\Delta\varphi$-TPD spectra are very useful in providing the continuous temperature dependence of the various reactive steps.

D. Deuterium Preadsorption. Preadsorption of deuterium serves as marker for the onset of methane formation and for surface passivation. In Figure 9 the surface passivation by deuterium is demonstrated by the molecular desorption following 1 ML adsorption of methyl bromide, which corresponds to 3.5 langmuirs exposure on the clean Ru(001) surface, (dotted line) and on a 0.9 ML deuterium precovered surface (solid line). On the deuterium-precovered surface, a new desorption peak grows at 140 K at exposures larger than 1.1 langmuir. The extent of dissociation is reduced from 50% on the clean Ru(001) surface down to 9% on the deuterium-precovered surface. In the inset of Figure 9, the Δp-TPD spectra following the exposure of the sample to 12 langmuirs of methyl bromide on the clean (dotted line) and on the 0.9 ML deuterium precovered surface (solid line) are shown. The peak that is attributed to the desorption from the second layer is shifted from 130 K on the clean Ru(001) surface to 140 K on the deuterium-precovered surface. As will be shown below, the dissociation onset of methyl bromide is around 125 K on the clean Ru(001) surface. Dissociation of first-layer molecules is expected to crowd the surface with bromine and methyl fragments. Most of the methyl fragments and the bromine atoms were found to be retained at the surface after the methyl bromide decomposition. As a result, surface sites are blocked and thus the interaction of the second-layer molecules with the Ru(001) surface is weakened, leading to lower desorption temperature. With considerably lower dissociation on the deuterium-precovered surface, a higher desorption temperature of the second layer is expected, consistent with our observation.

Δp-TPD spectra for masses 94 (CH_3Br), 17 (CH_3D), and 3 (HD), following exposure of 1.1 langmuirs of CH_3Br on various deuterium preadsorption coverages (indicated by monolayer units) are shown in Figure 10 a,b,c, respectively. Figure 10a demonstrates that up to 0.5 ML of deuterium the dissociation of the parent molecule resembles that of the bare metal although the distribution of products changes. At higher deuterium coverages the parent molecules desorb at 180−190 K, and the peak shifts to lower temperatures as coverage increases. This

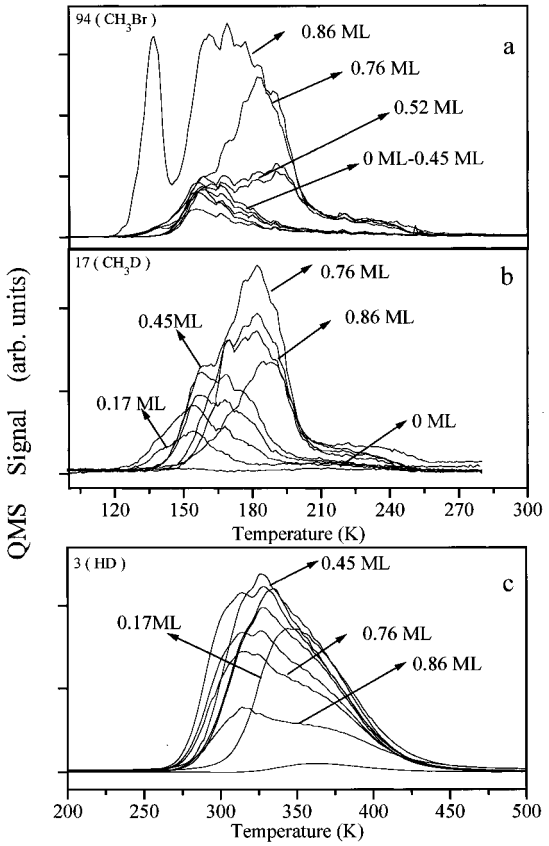

Figure 10. Δ*p*-TPD for (a) CH_3Br, (b) CH_3D, (c) HD after adsorption of 1.1 langmuirs of CH_3Br on deuterium-preadsorbed Ru(001) surface at the indicated deuterium coverages in units of monolayers (D/Ru = 1 ML at saturation deuterium coverage).

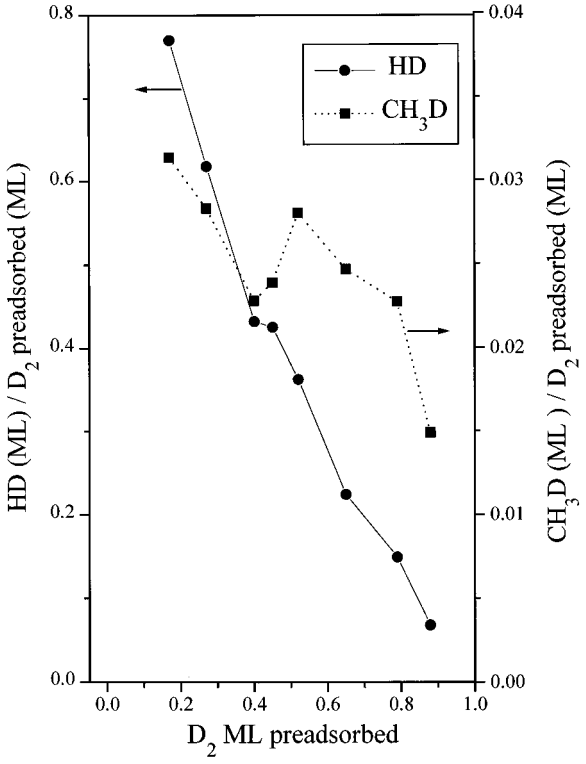

Figure 11. Uptake of HD, CH_3D normalized to the deuterium precoverage on Ru(001) calculated from data presented in Figure 10 b,c.

indicates that repulsion between neighbor molecules, which has been observed on the clean metal, exists on the deuterated surface as well. Moreover, while on the clean metal the desorption peak at 180−190 K appears only following exposures higher than 2.1 langmuirs of CH_3Br, in the presence of 0.5 ML of deuterium this peak is observable already at exposure of 1.1 langmuirs. This observation supports our understanding that deuterium acts mainly as a site blocker for direct contact of methyl bromide with the bare Ru surface atoms, thus suppressing dissociation .

In Figure 10b the rate of CH_3D production is shown. It goes through a maximum at deuterium coverage of 0.8 ML. Above this deuterium coverage the dissociation of methyl bromide rapidly decreases due to site blocking by the deuterium atoms. As a result, there are less methyl fragments on the surface and therefore the rate of formation of methane is slower as well. An interesting observation is that the maximum rate of CH_3D formation is shifted to higher temperatures as the deuterium coverage increases. This is contrary to the expectation for a second-order recombination reaction. However, in this case the competing routes of decreasing methyl coverage (less dissociation) with increasing deuterium coverage cause a net effect of decreasing rate of recombinative methane desorption. The same argument can be applied to explain the shift of the initial CH_3D production that signatures the onset of CH_3Br dissociation from 125 K at 0.17 ML of preadsorbed deuterium to 145 K at 0.75 ML of preadsorbed deuterium.

Figure 10c shows another indication for the decreasing dissociation via the formation and subsequent desorption of HD molecules (mass 3). The formation of HD is possible only after the methyl fragments further dissociate to CH_2 and H. The onset for this channel has been observed near 210 K from work function measurements, as discussed above. The fact that the maximum rate of production of HD is observed for deuterium precoverage of 0.45 ML while CH_3D production is maximized at 0.8 ML suggests that in the presence of deuterium not only the rate of the parent molecule's dissociation decreases but also that of the methyl fragments. Another reason for the maximum HD production rate at 0.45 ML deuterium precoverage is that a fraction of the methyl fragments desorb as methane at lower temperatures near 180 K (Figure 10b), which further diminishes the source of hydrogen atoms that should recombine at higher temperatures as HD.

The passivation of Ru(001) by deuterium preadsorption is summarized using the total Δ*p*-TPD uptake of the desorbing methyl bromide dissociation products. In Figure 11 the uptake of CH_3D and HD normalized to the precoverage of deuterium is shown. The total yield of HD and CH_3D reflects the probability of H(ad) or CH_3(ad) to encounter D(ad) and react. The fast, continuous reduction in the uptake of HD as D preadsorption increases directly reflects the slower rate of dissociation of the CH_3 fragments in the presence of D(ad). The second reason for this fast decay is the elimination of these methyl radicals as they recombine with D to desorb as CH_3D. The rate of formation of CH_3 radicals due to parent molecules dissociation (indicated by the uptake of CH_3D) slows down as well in the presence of deuterium. However, this channel is less sensitive to the coadsorbed deuterium; therefore the uptake of CH_3D diminishes at a slower rate than that of HD. The clear break in the rate of decay of both HD and CH_3D uptake at deuterium coverage near 0.5 ML is not quite well understood. It may relate to enhanced ordering of the preadsorbed deuterium at exactly half of a monolayer.

The passivation by hydrogen preadsorption reveals another interesting interplay between the two isotopes of hydrogen, D_2 and HD, while monitoring work function and TPD simultaneously. At deuterium coverages greater than 0.65 ML, the desorption peak shapes at masses 3 (HD) and 4 (D_2), following

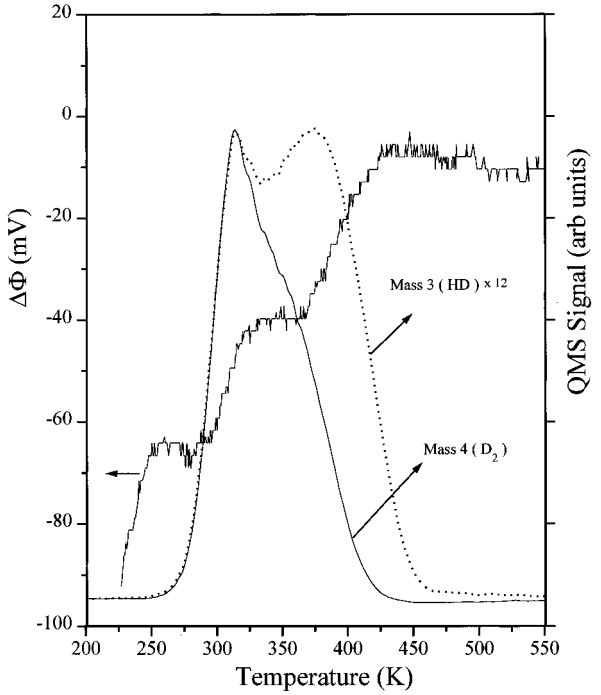

Figure 12. Δp-TPD signal of D_2 (mass 4) and HD (mass 3) and $\Delta\varphi$-TPD signal during dissociation of fragments originated from 8 langmuirs CH_3Br adsorbed on 0.9 ML of D_2 on Ru(001).

CH_3Br postadsorption of 0.33 ML, gradually change with a high-temperature shoulder emerging near 300 K at mass 3 only. In Figure 12 simultaneous Δp-TPD at m/e= 3 and 4 and $\Delta\varphi$-TPD are presented for a deuterium precoverage of 0.9 ML. The increase in work function of about 25 mV in the temperature range of 300−350 K follows precisely the desorption of D_2. The value of 25 mV is expected to represent the removal of 0.85 of the existing D atoms from a Ru(001) surface.[46] On the surface partially covered with bromine and hydrocarbon fragments this seems to reflect the desorption of only close to half of the remaining deuterium atoms that have not desorbed as CH_3D at lower temperatures; see Figure 10. Further heating to 400 K completes the desorption of D_2 molecules, but now HD is the primary desorbing species, with a peak desorption rate at 380 K. The sources for H atoms on the surface that can lead to HD desorption are CH(ad) and possibly also CH_2(ad) that have been stabilized up to these temperatures. The rate of decomposition of these species has been slowed in the presence of excess D(ad); therefore, we observe their enhanced decomposition via accelerated HD formation, just as the surface D coverage decreases around 350−380 K. The work function increase of 30 mV above 360 K, which coincides with HD desorption, reflects mainly the decomposition of hydrocarbon fragments, as seen in Figure 12.

Finally, surface passivation by deuterium has been employed to extract the absolute coverage of CH_3Br on Ru(001). Since on the fully deuterated surface the dissociation probability of the parent molecules is small, as indicated by the total HD uptake, we use this phenomenon to titrate the deuterium covered ruthenium atoms on the surface. This is done by monitoring the molecular CH_3Br desorption uptake as a function of deuterium preadsorption. The results are then extrapolated to zero deuterium-coverage to obtain the full monolayer coverage in the following way:

We define the coverage of CH_3Br on the clean or deuterated surfaces as $N_s\,\theta/\theta_s$, where N_s is the saturation density of methyl bromide molecules in the first layer and θ/θ_s is its fractional coverage. We assume the same unity sticking probability on the bare and the deuterated surfaces. Next we define $R(\theta_{CH_3Br})$ as the ratio of total uptake at mass 94 (CH_3Br) from the clean Ru to that obtained from the deuterated surfaces, at identical methyl bromide exposure for each of the deuterium precoverages studied. After correction is made for the dissociation on the fully deuterated surface, $[1-R(\theta_{CH_3Br})]$ is the fraction of dissociated methyl bromide molecules. This fraction is then experimentally obtained from the calibrated account of the density of CH_3 fragments observed on the surface as a function of deuterium precoverage. The total methyl density (defined as θ_{diss}) is obtained as a function of deuterium preadsorption from the total uptake of CH_4 and H_2. The coverage of H(ad) was calibrated by dosing hydrogen on clean Ru(001) and assuming that at saturation coverage H/Ru = 1.[40] We define $\theta_{diss} = \theta_{CH_4} + (\theta_{CH_4} + \theta_{H_2})/3$, because from every methyl three hydrogen atoms are formed and for each methane produced there are 1.33 methyl groups that are removed. All these are summarized as follows:

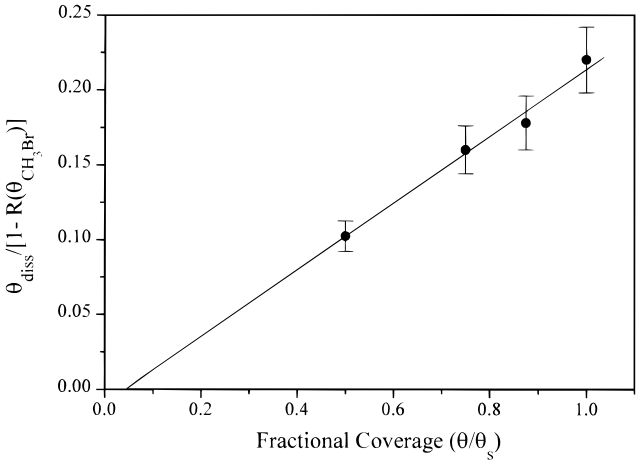

Figure 13. Plot of $\theta_{diss}/[1 - R(\theta_{CH_3Br})]$ vs the fractional coverage θ/θ_s of methyl bromide (see text).

$$N_s\theta/\theta_s\,[1 - R(\theta_{CH_3Br})] = \theta_{diss} \qquad (4)$$

The analysis discussed above is limited to a CH_3Br coverage range of 0.3−1.0 ML. The lower limit marks the termination of any further dissociation of methyl bromide on the deuterated surface as its coverage increases, and the upper limit is the completion of a monolayer. A plot of $\theta_{diss}/[1 - R(\theta_{CH_3Br})]$ vs the fractional coverage θ/θ_s should give the density N_s from the slope. This plot is shown in Figure 13 with a slope of 0.22, which should be understood as the density at monolayer methyl bromide coverage $CH_3Br/Ru = 0.22 \pm 0.02$, corresponding to $(3.6 \pm 0.3) \times 10^{14}$ molecules/cm^2 .

E. Br/Ru(001). Adsorption of halogens on metal surfaces has been studied extensively due to their technological significance.[31,32] On the basis of their large electron affinity, we would expect the work function of the metal to increase upon halogen adsorption. Indeed, in most of the systems that have been studied this is the case. However, examples do exist that show the opposite change in work function, e.g. Cl, Br, I /W(110), $\Delta\varphi = -0.26$, -0.32, and -0.78 V respectively.[47] Such behavior has also been predicted theoretically for Cl on Rh(001) with $\Delta\varphi = -0.1$ V.[48] Cl_2 and Br_2 decrease the work function on Pt(111) at low coverages, which is followed by an increase at higher coverages.[49,50]

After a sample saturated with a monolayer of methyl bromide is heated to 550 K (before $\Delta\varphi$ decreases due to the polymerization of carbon residues, see Figure 8), a 200 mV *decrease*

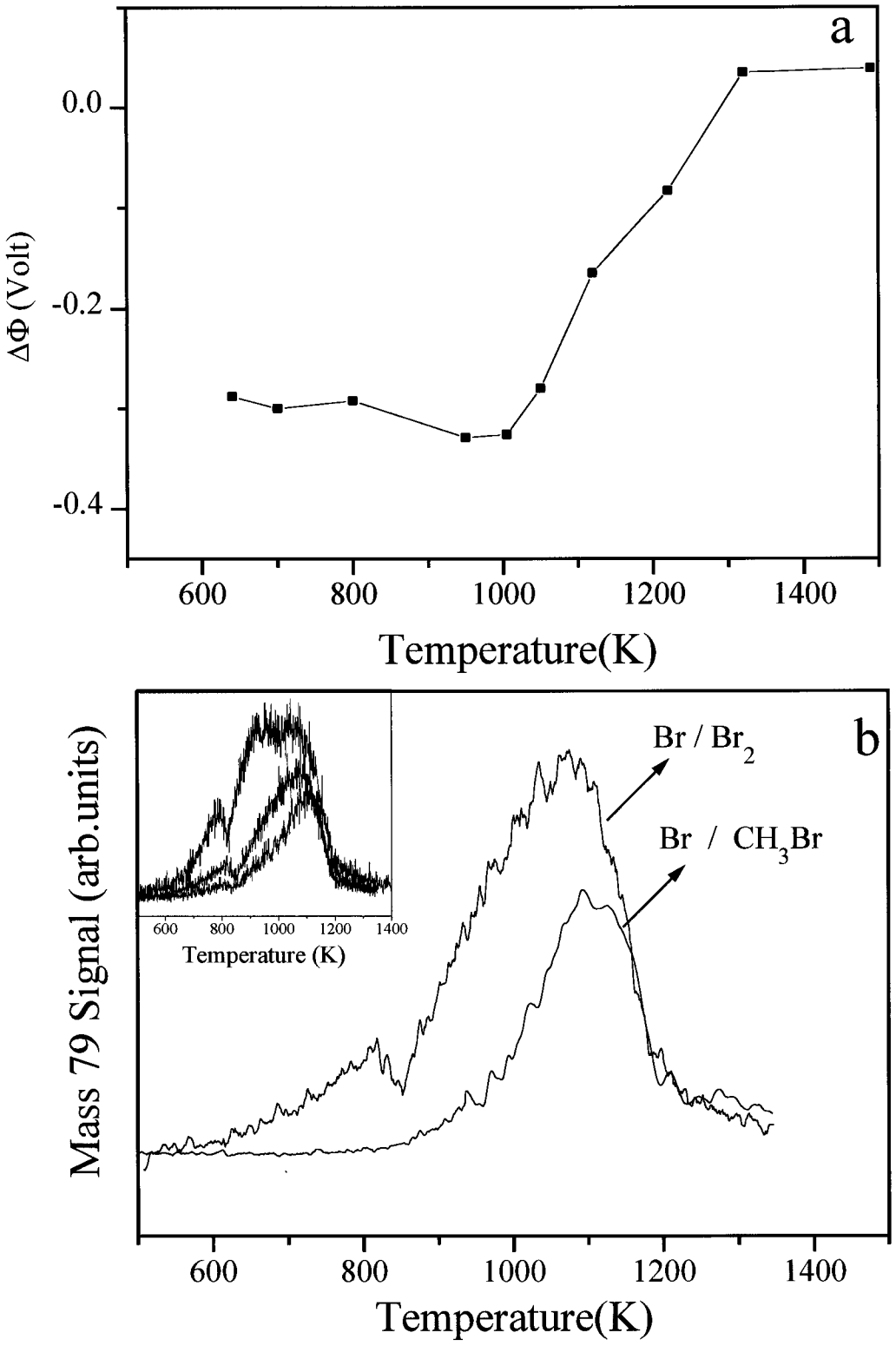

Figure 14. (a) Work function change upon desorption of Br atoms from Ru(001). (b) Δ*p*-TPD of Br either following the adsorption of Br_2 or as a result of CH_3Br thermal decomposition. In the inset Δ*p*-TPD spectra for increasing Br_2 exposures are presented.

in the work function relative to the bare metal is observed. Based on work function measurements of C_2H_4 on Ru(001),[44] the contribution of 0.1 ML of carbide on the surface is an *increase* of 200 mV. Thus, it is evident that bromine atoms that coadsorb with carbon adatoms decrease the work function of ruthenium upon adsorption. In order to substantiate this observation we used a 3 mm diameter doser to directly expose the sample to saturation coverage of Br_2 and then measured the work function and pressure increase in a TPD mode.

Upon adsorption of Br_2 on a Ru(001) surface held at 200 K the work function decreases by 650 mV. Annealing the sample to 600 K results in an increase in the work function by 300 mV, due to unknown weakly bonded bromine compounds. The work function change upon surface heating to temperatures higher than 600 K is shown in Figure 14a.

The Δ*p*-TPD in Figure 14b has a pronounced peak in the range 800−1200 K. This peak has been attributed to atomic Br desorption in other halogen−metal systems.[48,51,52] The work function increase due to the desorption of the atomic bromine is 320 mV, as seen in Figure 14a. A small desorption peak

near 800 K is responsible for a small increase in the work function ($\Delta\varphi$ slightly decreases upon its desorption).

The ratio of the integrated Δp-TPD signal obtained from the saturated layer of Br atoms and that from CH_3Br decomposition is 0.43 for saturation coverage of methyl bromide. On the basis of the estimate of methyl bromide saturation coverage discussed above, the bromine coverage that is associated with the high-temperature desorption peak at 1050 K is Br/Ru = 0.3 as obtained from the direct exposure to Br_2. The inset of Figure 14b shows the increasing desorption temperature as Br coverage decreases, a typical dipole−dipole repulsion effect.

A recent study of the Cl_2/Ru(001) system[53] has found that a Cl−$(\sqrt{3} \times \sqrt{3})R30°$ structure is formed at 1 mL and exclusively desorbs as atomic Cl. This observation correlates well with our assignment of the 0.3 ML coverage obtained from 1 ML of bromine on the Ru(001) surface, based on the calibration of the CH_3Br monolayer coverage. In the above study, if the chlorine coverage exceeds $^1/_3$ ML, more complex LEED patterns appear that are attributed to compressed Cl overlayer. This clarifies the nature of the 800 K bromine desorption as arising from the desorption of bromine atoms from a compressed overlayer.

At the final stage of decomposition of methyl bromide, carbon and bromine atoms are left on the surface. The separate contributions of each to the measured work function has been discussed above and was found to be of opposite sign: 0.11 ML of carbon *increases* $\Delta\varphi$ by 200 mV, and the same amount of bromine *decreases* the work function by 110 mV. The combined change is found to be nonadditive: A total *decrease* of 200 mV has been measured. We cannot explain this observation, except for the possibility that different sites with different contributions to the work function are populated in the coadsorption of methyl and bromine compared with separate adsorption of each of these species.

Atomic chlorine on Ru(100), which is a more open surface than the hexagonal close packed Ru(001), has been shown to increase the work function by 500 mV upon saturation adsorption.[51] We may learn from the opposing results of Cl/Ru(100) and Br/Ru(001) that simple concepts such as electron affinity are oversimplified for explaining the work function data. An explanation for the possibility that halogens will induce a decrease in work function upon adsorption on metal surfaces was discussed theoretically for the case of Cl on W(110).[48] It was argued that charge transfer from the metal to the adsorbed halogen, a configuration resembling that of rare gas Ar, is qualitatively obtained. The Ar-like closed shell thus repels the vacuum tail of the metallic charge distribution. This behavior is expected to work against net charge transfer to the halogen. This explanation may apply to the Br−Ru(001) system as well.

F. CH_3Br on Ru(001): $\Theta > 1$ ML. At coverages above a monolayer, new Δp-TPD peaks appear in the temperature range of 110−140 K, as seen in Figure 1. The β peak that can be assigned to the second-layer desorption grows at constant temperature near 129 K . The α' peak that starts to grow before the completion of the second layer near 119 K and another peak, α, which cannot be saturated, grows with a peak temperature near 126 K.

Above 4 ML (14 langmuirs of CH_3Br exposure), the population of the α' peak strongly decreases and it merges with the peak. In Figure 15 the Δp-TPD spectra of CH_3Br are shown together with those of CH_3I and CH_3Cl from Ru(001) for comparison. The difference in the chemistry of these molecules on Ru(001) is that CH_3I almost completely dissociates for coverages lower than 1 ML,[3,34] CH_3Br dissociates as well but with smaller probability (50%), as discussed in this report, but

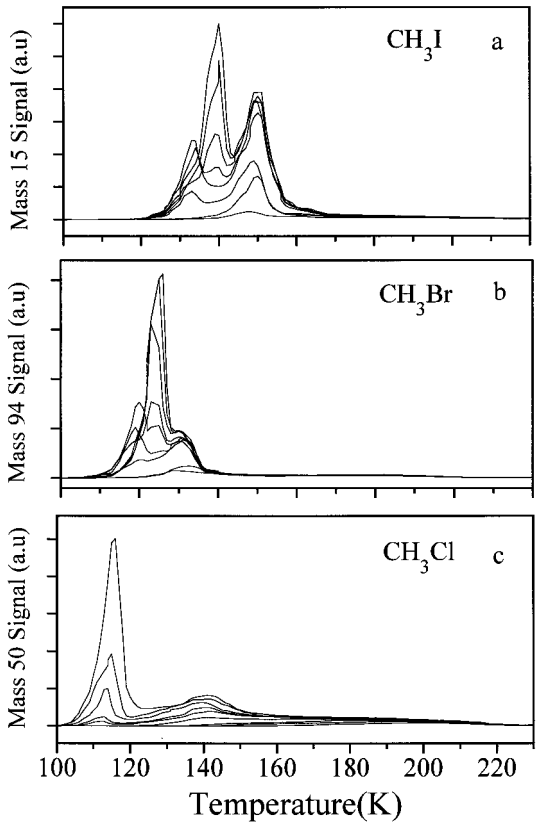

Figure 15. Δp-TPD of (a) CH_3I (mass 15), (b) CH_3Br (mass 94), and (c) CH_3Cl (mass 50) from Ru(001), adsorption temperature of 82 K, heating rate of 3 K/s.

CH_3Cl does not dissociate at all on Ru(001),[34] as on most transition metals. The appearance of a peak at lower temperature than the condensed layer peak for both CH_3I and CH_3Br is rather unusual. It implies a stabilization of the molecules that populate the α' peak by subsequent adsorption of methyl bromide molecules. The difference in the desorption temperature is not seen in the case of CH_3Cl.

Δp-TPD spectra with almost identical features were reported for CD_3I from TiO_2 (110) single crystal,[54] on which the molecules do not dissociate. This suggests that dissociation fragments play no important role in determining the observed Δp-TPD as a function of coverage. By correlating Δp-TPD and XPS measurements at low temperature, the multilayer peak for CD_3I/TiO_2(110) was suggested[54] to originate from molecules adsorbed at the second layer. Upon formation of three-dimensional (3D) islands by either increasing the coverage or rearrangement ("hopping" of a second-layer molecule to the third), the peak shifts to higher temperatures indicating stabilization of the second-layer by subsequent molecular adsorption. Adopting the above interpretation for the CH_3Br/Ru(001) system, the adsorption at the third-layer (with some adsorption at higher layers as well) is suggested to lead to a disordered structure. Since the work function decreases upon adsorption (see Figure 3) these molecules mostly adsorb with the bromine atoms pointing toward the surface. The integrated area of the α' peak was found to be 1.3 higher than the second-layer β peak. This indicates that the α' peak is populated by third-layer molecules possibly with higher density then the first two layers (weaker dipole−dipole interaction) while forming 3D islands. Due to the strong interaction with the Ru(001) surface, the dipoles at the third-layer are still forced to align nonrandomly (bromine down on the average) and the molecules arrange in a disordered structure.

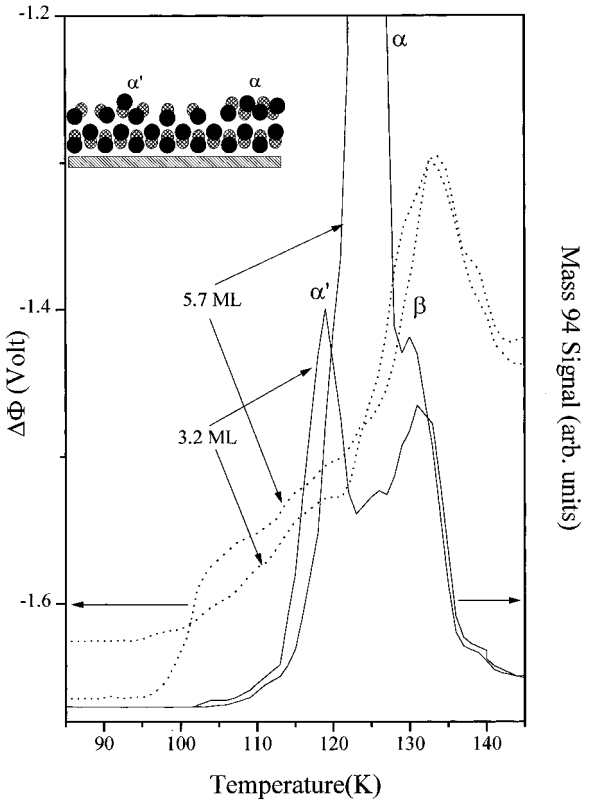

Figure 16. $\Delta\varphi$-TPD (dotted lines) and Δp-TPD (solid lines) after adsorption of 3.2 and 5.7 ML of CH_3Br on Ru(001) at 82 K. The heating rate was 2 K/s. In the inset a schematic view of the suggested structure of the first three CH_3Br layers on Ru(001) is shown.

The α' desorption peak shifts to higher temperatures as coverage increases. Within the narrow coverage range of 3.8−4.1 ML, α' merges with the α peak. A useful way to examine this peak's population change is to measure the work function change during surface heating. In Figure 16 a correlation between $\Delta\varphi$-TPD and Δp-TPD is shown at two different coverages: before and after the depletion of the α' peak. A sharp increase of 80 mV in the work function is seen between 95 and 106 K in $\Delta\varphi$-TPD for the high coverage followed by the onset of desorption of the α peak. This increase in the work function is suggested to arise from the rearrangement of a disordered structure into a well-organized bilayer-like packing that resembles the molecular crystalline.[21]

The first and second-layers were each found to consist of ca. 50% of the density of CH_3Br in the (001) plane of the molecular crystal, with the bromine facing the surface in the first layer and the methyl group facing the surface in the second layer. We use eq 1 to calculate the expected contribution of the second layer to the work function change if the first and the second-layers were decoupled, namely placing the second layer above the first and taking the distance of these CH_3Br molecules to be 6.4 Å, consistent with the relevant van der Waals radii.[29] The predicted contribution to the work function increase by the second-layer adsorption under the above assumptions is more than four times larger than the observed 0.3 V, considering a gas phase value for the isolated molecules' dipole moment at the second layer. Therefore, we conclude that the first and second layers must interact strongly to compensate for the net contribution of each of the layers. This interaction is attributed to opposing planes of dipoles that partially screen each other by forming a bilayer-like adsorption geometry. The distance from the surface of the methyl in the second layer is difficult to estimate and cannot be extracted from the work function data alone.

A schematic view of the model suggested above is shown in the inset of Figure 16. The first two layers are shown to form a "bilayer", having an antiparallel dipole configuration. Adsorption of third-layer molecules was shown to lead to a decrease of the work function. The orientation of these molecules, therefore, needs to be with the bromine facing the surface, but unlike the monolayer adsorption they are not expected to align normal to the surface due to the reduced interaction with the metal. Upon adsorption a 3D structure is formed with random dipole orientation above the third layer, suggested to desorb as the α' peak. However, heating the surface seems to lead to rearrangment of the multilayer structure into the stabilized antiparallel arrangement (second bilayer) that mimics the bulk methyl bromide crystalline structure.[21]

Unlike the case of CH_3Br and CH_3I, in CH_3Cl desorption from Ru(001) the low-temperature peak attributed to the condensed phase desorption is absent, as seen in Figure 15. The CH_3Cl crystal structure was found to be orthorhombic[55] with molecular dipoles ordered in the same direction inside the layer. As mentioned above, for the isomorphic CH_3Br and CH_3I, the molecular dipoles are arranged antiparallel.[21] This does not rule out the existence of disordered structure upon CH_3Cl adsorption on the Ru(001) surface, but it indicates that the difference in energy between the disordered and the crystalline structures is too small to detect in Δp-TPD. The extent of interaction of the molecule with the surface relative to the stabilization of the crystal structure formation is the important factor for the rearrangement of the molecules on the surface. Therefore, in the second-layer adsorption of CH_3Cl on Ru(001), the work function change is very similar to CH_3Br.[30] This means that the second-layer CH_3Cl molecules adsorb with the methyl pointing toward the surface, which is different from the crystalline structure.[55] The stabilization from lowering the dipole−dipole repulsion between molecules in the first-layer is the driving force for the second-layer adsorption geometry. However, at the third−fourth layers, in the absence of strong interaction with the surface, the stabilization upon crystal structure formation is the crucial factor.

IV. Conclusions

Work function measurements combined with TPD were employed to study the chemistry of CH_3Br on Ru(001) in the temperature range of 82−1350 K. Unique information on molecular and methyl fragment reactivity could be obtained at crystal temperatures below the onset for desorption. Monolayer coverage has been determined to be $(3.6 \pm 0.3) \pm 10^{14}$ molecules/cm^2, equivalent to $CH_3Br/Ru = 0.22 \pm 0.02$.

Strong dipolar lateral repulsion among neighbor CH_3Br molecules has been characterized in both work function and TPD data. The low-coverage dipole moment ($\mu_0 = 2.57$ D) and polarizability ($\alpha = 8.6 \times 10^{-24}$ cm^3) are larger than the corresponding gas phase values, resulting from the nature of interaction with the metal. These are attributed to molecules adsorbed with their C−Br bond axis perpendicular to the surface, with the bromine facing the metal. The increase in work function while heating, at temperatures prior to decomposition or desorption, has been discussed in terms of molecular rearrangements. These include a mechanism involving thermally activated flipping of a fraction of the molecules. The structure formed this way is similar to the geometry observed in the bulk crystalline methyl bromide−antiparallel packing of neighbor molecules.

The decomposition pathways of the methyl fragment could be determined by employing the differential work function mode, defining the temperature window for each of the

consecutive dehydrogenation steps. At higher coverages methane formation and desorption compete with the dehydrogenation of the methyl group. Deuterium preadsorption, which significantly passivates the surface, has been employed to better understand the various reactivity steps of the hydrocarbon fragments. Atomic bromine has been found to *decrease* the work function by 320 mV at a coverage of Br/Ru = 0.3, suggesting a complex charge redistribution upon adsorption.

Finally, work function measurements indicate the presence of strong interactions of the methyl bromide molecules with the metal surface up to the third-layer. Alternating contributions to the work function of the first three layers are observed. This is understood in terms of an opposite adsorption geometry in which bromine faces the surface at the first-layer, methyl at the second, and bromine again at the third. Upon heating, the third and fourth layers rearrange in a bilayer-like structure before the completion of the fourth-layer, leading to higher stability of the combined two layers compared with the third alone. This structure is rather similar to that of methyl bromide in its molecular crystal.

To conclude, the chemistry of methyl bromide on Ru(001) has been observed to fit well in the general reactivity trends of methyl halides on group VIII metal surfaces. The introduction of the various modes of work function measurements has significantly improved our ability to study fine details in the chemical reactivity of hydrocarbon fragments on reactive metal surfaces.

Acknowledgment. This research has been partially supported by a grant from the G.I.F., The German-Israeli Foundation for Scientific Research and Development, a grant from the European Economic Community together with the Israeli Science Ministry, and by the James Franck Program. The Farkas Center for Light Induced Processes is supported by the Bundesministerium für Forschung und Technologie and the Minerva Gesellschaft für die Forschung mbH.

References and Notes

(1) Chen, J. C.; Beebe, T. P., Jr.; Crowell, J. E.; Yates, J. T., Jr. *J. Am. Chem. Soc.* **1987**, *109*, 1726.
(2) Dubois, L. H.; Bent, B. E.; Nuzzo, R. G. *Surface Reactions* Madix, R. J., Ed. In Springer Series in Surface Science 34; Springer Verlag: Berlin, **1994**; Chapter 5, p 135.
(3) Zhou, Y.; Henderson, M. A.; Feng, W. M.; White, J. M. *Surf. Sci.* **1989**, *224*, 386.
(4) Henderson, M. A.; Mitchell, G. E.; White, J. M. *Surf. Sci. Lett.* **1987**, *184*, L325.
(5) Liu, Z.-M.; Costello, S. A.; Roop, B.; Coon, S. R.; Akhter, S.; White, J. M. *J. Phys.Chem.* **1989**, *93*, 7681.
(6) Zaera, F.; Hoffmann, H. *J. Phys. Chem.* **1991**, *95*, 6297.
(7) French, C.; Harrison, I. *Surf. Sci.* **1995**, *342*, 85.
(8) French, C. ; Harrison, I. *Surf. Sci.*, submitted.
(9) Chen, J.-J.; Winograd, N. J. *Surf. Sci.* **1994**, *314*, 188.
(10) Jenks, C. J.; Lin, J.-L.; Chiang, C.-M.; Kang, L.; Leang, P. S.; Wentzlaff, T.H.; Bent, B. E. *Structure-Activity and Selectivity Relationships in Heterogeneous Catalysis*; Grasseli, R. K., Sleight A. W., Eds.; Elsevier: Amsterdam, 1991, p 301.
(11) Lamont, C. L. A.; Conrad, H.; Bradshaw, A. M. *Surf. Sci.* **1993**, *280*, 79.
(12) Chiang, C.-M.; Wentzlaff, T. H.; Jenks, C. J.; Bent, B. E. *J. Vac. Sci. Technol.* **1992**, *A10*, 2185.
(13) Lin, J.-L.; Chiang, C.-M.; Jenks, C. J.; Yang, M. X.; Wentzlaff, T. H.; Bent, B.E. *J. Catal.* **1994**, *147*, 250.
(14) Zhou, X.-L.; Solymosi, F.; Blass, P. M.; Cannon, K. C.; White, J. M. *Surf. Sci.* 1**989**, *219*, 294.
(15) Zhou, X.-L. ; White, J. M. *Surf. Sci.* **1991**, *241*, 244, 259, 270.
(16) Marsh, E. P.; Tabares, F. L.; Schneider, M. R.; Gilton, T. L.; Meier, W.; Cowin, J. P. *J. Chem. Phys.* **1990**, *92* (3), 2004.
(17) Bent, B. E. *Chem Rev.* **1996**, *96*, 1361.
(18) Pfnür, H.; Feulner, P.; Menzel, D. *J. Chem. Phys.* **1983**, *79* (9), 4613.
(19) Feulner, P.; Menzel, D. *Phys. Rev. B* **1982**, *25* (6), 4295
(20) Lu, P.-H.; Lasky, P. J.; Yang, Q.-Y.; Wang, Y.; Osgood, R. M., Jr. *J. Chem. Phys*. **1994**, *101* (11), 10145.
(21) Kawaguchi, T.; Hijikigawa, M.;Hayafuji, Y.; Ikeda, M.; Fukushima, R.; Tomiie, Y. *Bull. Chem. Soc. Jpn.* **1973**, *46*, 53.
(22) Berko, A.; Erley, W.; Sander, D. *J. Chem. Phys*. **1990**, *93*, 8300.
(23) Topping, J. *Proc. R. Soc. London* **1927**, *A114*, 67.
(24) Heras, J. M.; Albano, E. V. *Z. Phys. Chem. Neue Folge* **1981**, *126*, 57.
(25) Albano, E. V. *Appl. Surf. Sci.* **1982**−**83**, *14*, 183.
(26) Albano, E. V. *J. Chem. Phys.* **1985**, *85* (2), 1044.
(27) Maschhoff, B. L.; Ledema, M. J.; Cowin, J. *Surf. Sci.* **1996**, *359*, 253.
(28) Maschhoff, B. L.; Cowin, J. *J. Chem. Phys.* **1994**, *101* (9), 8138.
(29) Pauling, L. In *The Nature of the Chemical Bond*, 3rd ed.; Cornell University Press: Ithaca, NY, 1960; pp 260.
(30) Livneh, T.; Asscher, M. Unpublished results.
(31) Grunze, M.; Dowben, P. A. *Appl. Surf. Sci*. **1982**, *10*, 209.
(32) Jones, R. J. *Prog. Surf. Sci*. **1988**, *27* (1/2).
(33) Lang, N. D. *Surf. Sci.* **1994**, *299/300*, 284.
(34) Livneh, T.; Asscher, M. *Surf. Sci.*, submitted.
(35) Lin, J.-L.; Bent, B. E. *J. Phys. Chem.* **1993**, *97*, 9713.
(36) Doering, D. L.; Semancik, S.; Madey, T. E. *Surf. Sci.* **1983**, *133*, 49.
(37) Bonzel, H. P.; Pirug, G.; Müller, J. E. *Phys. Rev. Lett*. **1987**, *58*, 2138.
(38) Bonzel, H. P.; Pirug, G.; Ritke, C. *Langmuir* **1991**, *7*, 3006.
(39) Holbert, V. P.; Garrett, S. J.; Stair, P. C.; Weitz, E. *Surf. Sci.* **1996**, *346*, 189.
(40) Lindroos, M.; Pfnür, H.; Feulner, P.; Menzel, D. *Surf. Sci.* **1987**, *180*, 237.
(41) Barteau, M. A.; Broughton, J. Q.; Menzel, D. *Appl. Surf. Sci*. **1984**, *19*, 92.
(42) Hills, M. M.; Parmeter, J. E; Mullins, C. B.; Weinberg, W. H. *J. Am. Chem. Soc.* **1986**, *108*, 3554.
(43) Henderson, M. A.; Mitchell, G. E.; White, J. M. *Surf. Sci.* **1988**, *203*, 378.
(44) Livneh, T.; Asscher, M., in preperation.
(45) Lauderback, L. L.; Delgass, W. H. *Surf. Sci.* **1986**, *172*, 715.
(46) Feulner, P.; Menzel, D. *Surf. Sci.* **1985**, *154*, 465.
(47) Jowett, C. W.; Hopkins, B. J. *Surf. Sci.* **1970**, *22*, 392.
(48) Feibelman, P. J.; Hamann, D. R. *Surf. Sci.* **1985**, *149*, 48.
(49) Erley, W. *Surf. Sci.* **1980**, *94*, 281.
(50) Bertel, E.; Schawaha, K.; Netzer, F. P. *Surf. Sci.* **1979**, *83*, 439.
(51) Gudde, N. J.; Lambert, R. M.; *Surf. Sci.* **1983**, *134*, 703.
(52) Tysoe, W. T.; Lambert, R. M.; *Surf. Sci.* **1982**, *115*, 37.
(53) Preyss, W.; Ebinger, H. D.; Fick, D.; Polenz, C.; Polivka, B.; Saier, V.; Veith, R.; Weindel, Ch.; Jänsch, H. J. *Surf . Sci.* **1997**, *373*, 33.
(54) Garrett, S. J.; Holbert, V. P.; Stair, P. C.; Weitz, E. *J. Chem. Phys.* **1994**, *100*, (6) 4615.
(55) Burbank, R. D. *J. Am. Chem. Soc.* **1953**, *75*, 1211.